Simulation of phonon-assisted band-to-band tunneling in carbon nanotube field-effect transistors

Siyuranga O. Koswatta, Mark S. Lundstrom, M. P. Anantram, and Dmitri E. Nikonov
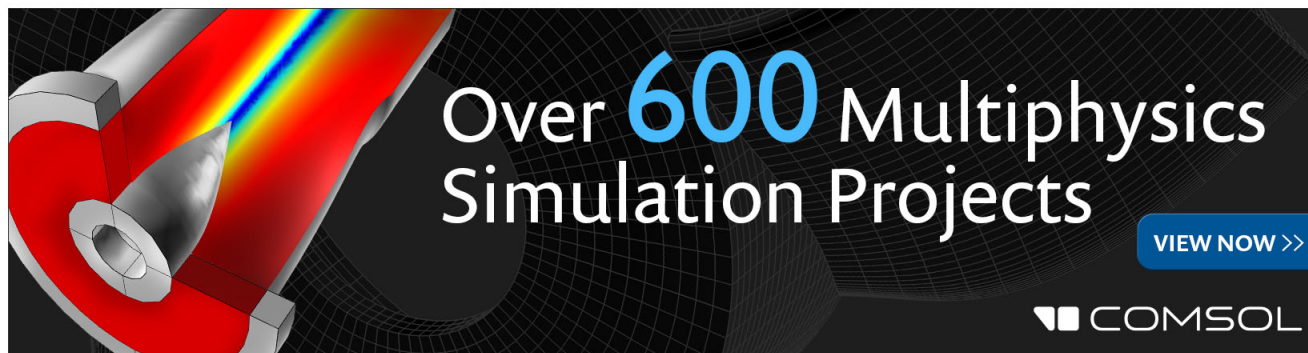

Articles you may be interested in

An efficient atomistic quantum mechanical simulation on InAs band-to-band tunneling field-effect transistors
Appl. Phys. Lett. **104**, 123504 (2014); 10.1063/1.4869461

Joule heating and thermoelectric properties in short single-walled carbon nanotubes: Electron-phonon interaction effect
J. Appl. Phys. **110**, 124319 (2011); 10.1063/1.3671069

Non-equilibrium Green's function analysis of cross section and channel length dependence of phonon scattering and its impact on the performance of Si nanowire field effect transistors
J. Appl. Phys. **110**, 094518 (2011); 10.1063/1.3658856

A tunneling field-effect transistor exploiting internally combined band-to-band and barrier tunneling mechanisms
Appl. Phys. Lett. **98**, 123504 (2011); 10.1063/1.3569760

Effect of intravalley acoustic phonon scattering on quantum transport in multigate silicon nanowire metal-oxide-semiconductor field-effect transistors
J. Appl. Phys. **108**, 034510 (2010); 10.1063/1.3457848

Simulation of phonon-assisted band-to-band tunneling in carbon nanotube field-effect transistors

Siyuranga O. Koswatta and Mark S. Lundstrom
School of Electrical and Computer Engineering, Purdue University, West Lafayette, Indiana 47907-1285

M. P. Anantram
Center for Nanotechnology, NASA Ames Research Center, Mail Stop 229–1, Moffett Field, California 94035-1000

Dmitri E. Nikonov[a)]
Technology and Manufacturing Group, Intel Corp., SC1-05, Santa Clara, California 95052

Electronic transport in a carbon nanotube metal-oxide-semiconductor field effect transistor (MOSFET) is simulated using the nonequilibrium Green's functions method with the account of electron-phonon scattering. For MOSFETs, ambipolar conduction is explained via phonon-assisted band-to-band (Landau–Zener) tunneling. In comparison to the ballistic case, we show that the phonon scattering shifts the onset of ambipolar conduction to more positive gate voltage (thereby increasing the off current). It is found that the subthreshold swing in ambipolar conduction can be made as steep as 40 mV/decade despite the effect of phonon scattering. © *2005 American Institute of Physics*. [DOI: 10.1063/1.2146065]

Electronic transport in conventional metal-oxide-semiconductor field-effect transistors (MOSFETs) is limited at room temperature primarily by surface roughness and phonon scattering. However carbon nanotubes (CNTs), due to their high mobility, are believed to be operating in the ballistic regime under low source-drain bias. CNT field effect transistors (FETs) (Refs. 1–4) have been recently demonstrated. Nonequilibrium Green's function simulations of carbon nanotubes[5,6] have been performed in the ballistic limit. It was demonstrated that the simulation results are in good agreement with experiments[7] at least over a wide range of parameters. Monte Carlo simulations[8] showed that in some regimes scattering produces only a small effect on current.

In this letter, we introduce into the formalism a model of scattering due to electron-phonon interaction and explore the range of validity of the previous quasi-ballistic results. We show that the most dramatic difference occurs for the off current, i.e., at the cross over from the direct (over the barrier) conduction to ambipolar (tunneling) conduction. Ambipolar conduction is a well-understood effect in CNT Schottky-barrier FETs.[9] We show that it also occurs in CNT MOSFETs. The effects of band-to-band (Landau–Zener) tunneling[10] in CNTFETs have been experimentally investigated by Appenzeller *et al.*[11] Here, we examine ambipolar conduction in the presence of phonon scattering. We explore the physics of the very steep subthreshold swing in ambipolar conduction as recently reported by Appenzeller *et al.*[11] We describe regimes where it is preserved or destroyed by phonon scattering.

We apply the nonequilibrium Green's functions method, as described by Datta[12] to simulation of the carbon nanotube transistors and extend the method of Refs. 5,6. It involves solution of the equation for the Green's function, G, in the mode-space approach[13]

$$(EI - H - \Sigma)G(E) = I, \qquad (1)$$

where E is the energy of quantum states, the imaginary part of self-energy, $\Sigma = -i(\Sigma^{in} + \Sigma^{out})/2$, contains the contribution of, respectively, in- and outscattering and contacts. Here, we disregard the real part of the phonon scattering self-energy. The Hamiltonian, H, of the device includes the tight-binding coupling between carbon atoms with the hopping parameter, $t = 3$ eV, at the nearest-neighbor distance, $a_{cc} = 0.142$ nm, as well as the electrostatic potential energy. The latter is expressed via the potential, V, from a solution of the Poisson's equation with electric charges given by the electron and hole densities, n and p, respectively; see Refs. 5,6 for the geometry of the device and the details of the computation. The carrier densities are obtained via integrals over energy of the electron and hole correlation functions,

$$G^n = G\Sigma^{in}G^+, \quad G^p = G\Sigma^{out}G^+; \qquad (2)$$

they express the density of filled and unfilled states, respectively, over the energy and the coordinate. All the G functions are matrices in the basis of the discrete points, x, along the nanotubes and were calculated using the efficient algorithm presented in Ref. 14. We will be plotting the energy spectrum of the current, calculated according to Ref. 14.

In addition to commonly included contributions to self-energy from the source and drain electrodes, here we also introduce the contributions due to electron-phonon scattering

$$\Sigma^{in}(E) = R_{ph}[(N_\omega + 1)G^n(E + \hbar\omega) + N_\omega G^n(E - \hbar\omega)], \qquad (3)$$

$$\Sigma^{out}(E) = R_{ph}[(N_\omega + 1)G^p(E - \hbar\omega) + N_\omega G^p(E + \hbar\omega)], \qquad (4)$$

where the diagonal elements of the electron and hole correlation functions are implied, the energy of a phonon mode is $\hbar\omega$, number of phonons in a mode, N_ω, is given by the Bose–Einstein distribution. The electron-phonon coupling constant, R_{ph}, for an $(n, 0)$ zig-zag CNT is determined by the matrix element[15] of the deformation potential D_0 and the carbon atom mass m_C $R_{ph} = \hbar D_0^2 / nm_C\omega$. In this letter for simplic-
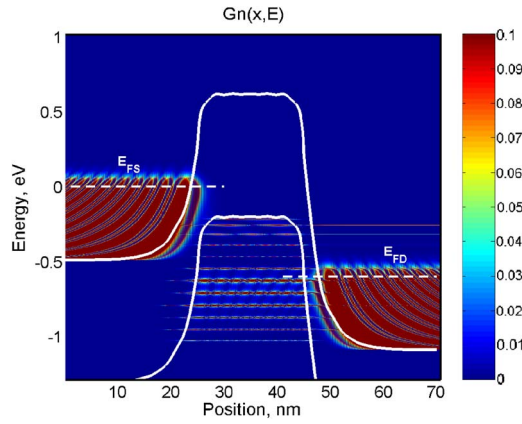
[a)]Electronic mail: dmitri.e.nikonov@intel.com

FIG. 1. (Color online) Distribution of electrons over energies in the CNT without phonon scattering; $Vg=-0.55$ V, $V_d=0.6$ V, source/drain doping 1.5×10^9 /m. White curves are the positions of the conduction (higher) and the valence (lower) band edges.

ity, we approximate the optical phonons by the fixed energy, 160 meV, and the coupling constant, 0.03 (eV)^2, independent of phonon momentum. We model a CNTFET with a (n,m) $=(13,0)$ CNT surrounded by a gate in a cylindrically symmetric geometry. The bandgap energy for this nanotube is, $E_g\approx0.82$ eV. The gate dielectric is HfO$_2$ with dielectric constant $\varepsilon=16$ and thickness of 2 nm. Source and drain are n doped to linear density, N_d, the channel of 20 nm in length is undoped. The doping density for the results in Figs. 1–3 is $N_d=1.5\cdot10^9$/m and in Fig. 4 it is $N_d=6\times10^8$/m. This is to be compared with the linear density of carbon atoms of N_{at} $=4n/(3a_{cc})=1.2\times10^{11}$/m for this size of the nanotube. The contacts to the gate and the ends of source and drain are assumed to be infinite reflectionless reservoirs; bias voltages V_g and V_d are applied to them. We calculate the distribution of free carriers and the current along the carbon nanotubes. All the results in this letter are for the temperature of 300 K. The simulation results for the electron occupation, $G^n(x,x,E)$, in states with a certain energy along the nanotube are presented in Fig. 1 for the ballistic case, and in Fig. 2 for the case with phonon scattering. The source (left) and the drain (right, in Fig. 1) are filled with electrons up to the Fermi level. For the drain, the Fermi level is shifted downward due to the applied bias. Electrons occupy the states in the conduction band, but some electron density in the band gap is also observed and corresponds to the evanescent tails
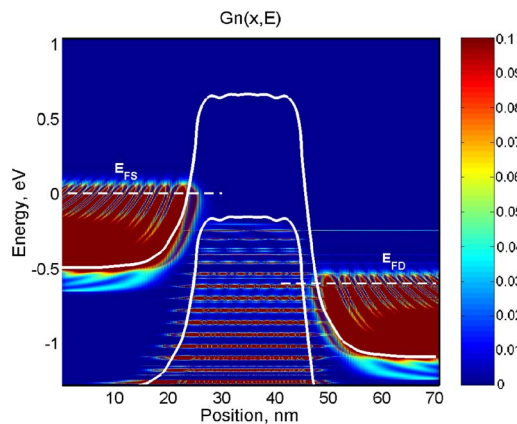

FIG. 2. (Color online) Distribution of electrons with phonon scattering $R_{ph}=0.03(eV)^2$; other parameters same as in Fig. 1.
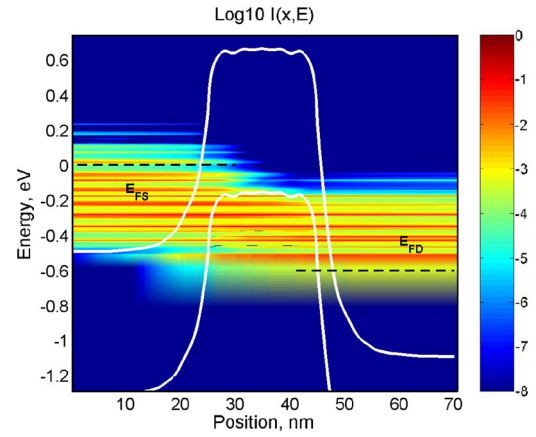

FIG. 3. (Color online) Current spectrum (logarithmic scale) with phonon scattering. Parameters same as in Fig. 2.

of the wave functions. The negative gate bias forces the conduction and valence band in the channel to be at higher energy. The holes in the channel are confined by the barrier formed by borders with the source and drain. For sufficiently short length of the channel, discrete states corresponding to longitudinal confinement are formed; they are clearly seen in the electron distribution in Figs. 1 and 2.

The current distribution over energies (not shown here) is position independent in the ballistic case. Current flows by electron tunneling from the conduction band, to the discrete states in the valence band and then by tunneling to the empty states in the conduction band of the drain (as shown by peaks of electron density there). The changes brought by the inclusion of phonon scattering (Fig. 2) are as follows. Electron density is noticeable in the band gap at approximately a value of energy of one phonon below the band edge in the source and drain. These are quasi-continuous virtual states caused by scattering, where electrons remain over the time sufficient to tunnel to the valence band. A discrete state [which would be better noticeable in the hole distribution $G^p(x,x,E)$] is formed at a value of energy of one phonon above the valence band in the channel. These phenomena bear a close similarity with those in resonant tunneling devices.[16,17]

This insight into the processes governing conduction is confirmed by the current distribution (Fig. 3). It has a series of sharp peaks each corresponding to a discrete state in the channel. As the coordinate varies from the source to the drain, the current distribution shifts to lower energies due to emission of phonons. Uninterrupted lines of current distribution correspond to a fraction of electrons tunneling without
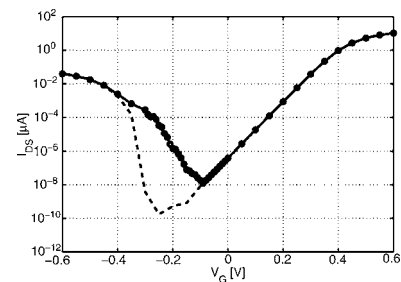

FIG. 4. Current vs gate voltage, for $V_d=0.1$: Without scattering (dashed line); with phonon scattering (solid line with circles). The doping density is 6×10^8/m.

scattering. Lines ending in the channel are explained by tunneling with a subsequent emission of a phonon. Lines starting in the band gap show electrons first emitting phonons and then tunneling to lower energy discrete states.

The effect of the phonon scattering is most visible in the dependence of the current on gate voltage, Fig. 4. The current–voltage (*I-V*) characteristics in the ballistic approximation (dashed line) and with phonons (solid line) are close for large positive or negative values of gate voltage, in agreement with the results of a semiclassical Monte Carlo simulation.[8] For the positive gate voltage, the current saturates when the potential barrier formed by the channel is low enough for all available carriers to flow without reflection. The current decreases with voltage with a subthreshold swing approximately 60 mV/decade as expected for an over-the-barrier flow due to the tail of the Fermi distribution. Current increases again at negative gate biases when tunneling conduction comes into play. It happens when the top of the valence band in the channel aligns in energy with the bottom of the conduction band in the source. Another condition is that unoccupied states in the drain are available at this energy. The current saturates at large negative gate voltages when a sufficient number of discrete states are aligned to energies to transport carriers from source states that are filled to the drain states that are empty. Note that a large current $\sim 1~\mu A$ can be achieved through tunneling for sufficiently large drain bias and doping.

The difference between the ballistic limit and phonon scattering is most pronounced at small gate voltages, at the cross over between the over-the-barrier current and tunneling current. The onset of tunneling conduction is shifted to more positive gate biases. The reason for that is that conduction is possible with emission of a phonon when the top of the valence band in the channel is at a lower energy than the bottom of the conduction band in the source. This is in agreement with the fact that the shift in voltage is approximately equal to the energy of a phonon. Our simulations show existence of a steep (<60 mV/decade at room temperature) subthreshold swing in the *I-V* curve in the ambipolar conduction region. The turn on of this conduction with the change of the gate voltage happens due to overlap of the discrete states and a band edge. Thus, it is not limited by the slope of the tail of the Fermi distribution. In Fig. 4, the swing in the ballistic regime is 25 mV/decade around $Vg=-0.3$ V. With phonon scattering, the swing is 40 mV/decade for Vg between -0.3 and -0.14 V.

Note that this situation changes with the doping density and, consequently, the Fermi-level energy in the source relative to the band edge, F_s. It determines the on-off current ratio approximately as $\exp((E_g-F_s)/(k_BT))$. For higher doping, the on-off current ratio is lower, and the steep subthreshold swing exists in the ballistic approximation but disappears in the presence of phonon scattering. For example, for $N_d = 1.5 \times 10^9$ /m, a steep subthreshold swing is 26 mV/decade at $Vg=-0.1$ is seen in the ballistic limit, while with phonon

scattering it never exceeds 140 mV/decade. The reason is that in all cases, the turn on of ambipolar conduction is less sharp than one expects from the ballistic calculations: Smaller contribution to conduction exist at higher gate voltages when multiphonon scattering becomes resonant with discrete states.

These results have significant consequences for the device design. One has to include phonon scattering to get the correct value of the gate voltage, at which the current is minimal, and to predict its exact value. In the presence of phonon scattering, one can obtain a sharp turn on of current in ambipolar conduction, but at lower doping density and consequently smaller "on" current.

In summary, we demonstrated that the ambipolar conduction in CNTs is ruled by phonon-assisted band-to-band tunneling. Phonon scattering shifts the onset of ambipolar conduction to more positive gate voltage and thereby sets a lower limit for the off current. The steep subthreshold swing expected in tunneling conduction occurs for lower doping of the source and drain and is destroyed by phonon scattering for higher doping levels.

[1]S. J. Tans, A. R. M. Verschueren, and C. Dekker, Nature (London) **393**, 49 (1998).

[2]S. Heinze, J Tersoff, R. Martel, V. Derycke, J Appenzeller, and P. Avouris, Phys. Rev. Lett. **89**, 106801 (2002).

[3]J. Appenzeller, J. Knoch, V. Derycke, R. Martel, S. Wind, and P. Avouris, Phys. Rev. Lett. **89**, 126801 (2002).

[4]A. Javey, J. Guo, Q. Wang, M. Lundstrom, and H. Dai, Nature (London) **424**, 654 (2003).

[5]J. Guo, S. Datta, and M. Lundstrom, IEEE Trans. Electron Devices **51**, 172 (2004).

[6]J. Guo, S. Datta, M. Lundstrom, and M. P. Anantram, Int. J. Multiscale Comput. Eng. **2**, 257 (2004).

[7]A. Javey, J. Guo, D. B. Farmer, Q. Wang, E. Yenilmez, R. G. Gordon, M. Lundstrom, and H. Dai, Nano Lett. **4**, 1319 (2004).

[8]J. Guo and M. Lundstrom, Appl. Phys. Lett. **86**, 193103 (2005).

[9]R. Martel, V. Derycke, C. Lavoie, J. Appenzeller, K. K. Chan, J. Tersoff, and P. Avouris, Phys. Rev. Lett. **87**, 256805 (2001).

[10]L. D. Landau and E. M. Lifshitz, *Quantum Mechanics: Nonrelativistic Theory*, 3rd ed. (Butterworth–Heinemann, London, 1981), Chap. VII.

[11]J. Appenzeller, Y.-M. Lin, J. Knoch, and P. Avouris, Phys. Rev. Lett. **93**, 196805 (2004).

[12]S. Datta, *Quantum Transport: Atom to Transistor*, 2nd ed. (Cambridge University Press, Cambridge, MA, 2005).

[13]R. Venugopal, Z. Ren, S. Datta, M. S. Lundstrom, and D. Jovanovic, J. Appl. Phys. **92**, 3730 (2002).

[14]A. Svizhenko, M. P. Anantram, T. R. Govindan, B. Biegel, and R. Venugopal, J. Appl. Phys. **91**, 2343 (2002).

[15]G. D. Mahan, Phys. Rev. B **68**, 125409 (2003).

[16]N. S. Wingreen, K. W. Jacobsen, and J. W. Wilkins, Phys. Rev. Lett. **61**, 1396 (1988).

[17]L. I. Glazman and R. I. Shekhter, Solid State Commun. **66**, 65 (1988).